Regular Article

Hydrogen-enhanced orientation dependence of stress relaxation and strain-aging in Hadfield steel single crystals

E.G. Astafurova [a,*], V.A. Moskvina [b], G.G. Maier [a], E.V. Melnikov [a], G.N. Zakharov [a], S.V. Astafurov [a], H.J. Maier [c]

[a] Institute of Strength Physics and Materials Science SB RAS, 2/4 Akademichesky ave., 634055 Tomsk, Russia
[b] National Research Tomsk Polytechnic University, 30 Lenin ave., 634050 Tomsk, Russia
[c] Institut für Werkstoffkunde (Materials Science), Leibniz Universität Hannover, An der Universität 2, 30823 Garbsen, Germany

ABSTRACT

The effects of electrochemical hydrogen charging on the stress relaxation and strain-aging of $\langle 111 \rangle$ - and $\langle 001 \rangle$ - oriented single crystals of Hadfield steel were studied under tension at room temperature. An orientation dependence of stress relaxation and strain-aging-assisted yield-drop phenomena was observed for hydrogen-free $\langle 111 \rangle$ - and $\langle 001 \rangle$ - oriented single crystals. Hydrogen charging up to five hours increased the stress relaxation rate for slip-associated deformation in $\langle 001 \rangle$ -oriented single crystals and decreased it for twinning-assisted deformation in $\langle 111 \rangle$ -oriented specimens. The present results demonstrate that different mechanisms dominate the interaction of hydrogen with dislocations, stacking faults and twins.

© 2017 Acta Materialia Inc. Published by Elsevier Ltd. All rights reserved.

Stable austenitic steels are attractive materials for various applications that envolve hydrogen environments. The austenite stability is considered to be one of the most important criterions for high resistance of the steel to hydrogen embrittlement (HE) [1–2]. However, using seven stable austenitic Cr-Ni, Cr-Ni-Mn-N, Mn-C, Mn-Al-C, and Cr-Mn-N steels with different stacking fault energies, deformation modes and levels of interstitial solution hardening, Michler and co-authors [3] found that austenite stability is not a sufficient parameter to predict HE resistance. Moreover, the tensile ductility of hydrogen saturated steel can be degraded even in the absence of α′-martensite. They suggested that stable steels, which deform homogeneously, are more resistant to hydrogen-assisted fracture than steels, which demonstrate localized deformation, in particular, planar slip or mechanical twinning. A similar conclusion was made by Phaniraj et al. [1] for hydrogen-saturated 18Cr10Mn0.6N austenitic steel, which does not undergo a γ → α′ martensitic transformation under plastic deformation. Solute hydrogen is known to increase slip planarity [4–5] and cause HE due to hydrogen-enhanced localized plasticity (HELP) [6–8]. Deformation twinning has been also reported to be an important factor for hydrogen-induced cleavage-like fracture [3,9–12]. For single crystalline type 316 austenitic stainless steel, M. Koyama et al. [10] reported that deformation twin density and the morphologies of deformation twins all contribute to

the hydrogen embrittlement process. As hydrogen stimulates both effects (twinning and HELP) for steels, additional experimental and theoretical research on the effect of hydrogen on dislocation activity and other deformation mechanisms is needed.

In the present study, single crystals were employed for analyzing the elementary dislocation processes responsible for plastic deformation, stress relaxation and strain aging under hydrogen-free and hydrogen-saturated conditions. Depending on the crystal orientation different deformation mechanisms (slip and twinning) are favored at ambient temperature and low strain. The objective was to study the effect of electrochemical hydrogen charging on the stress relaxation and strain-aging of $\langle 111 \rangle$ - and $\langle 001 \rangle$ - oriented single crystals of Hadfield steel under tension at room temperature. Specifically, the study was designed to address the following issues.

1) The effect of orientation on stress relaxation and strain aging in the uncharged condition. This orientation dependence results from the effect of applied stresses on $a/2 \langle 110 \rangle$ dislocation splitting, which in turn results in different deformation mechanism. For $\langle 001 \rangle$ -oriented crystals slip dominates and a homogeneous dislocation arrangement results. In case of $\langle 111 \rangle$ -oriented crystals, twinning and slip is favored. For details see Refs [13–16].

2) The influence of hydrogen charging on the elementary dislocation processes. Specifically, the cases of full $a/2 \langle 110 \rangle$ dislocations, $a/2 \langle 110 \rangle$ dislocations splitted into two $a/6 \langle 211 \rangle$ partials and $a/6 \langle 211 \rangle$ partial dislocations were addressed. The latter, are important in the context of stacking fault and twin formation, respectively.

* Corresponding author at: Laboratory of Physics of Structural Transformations, Institute of Strength Physics and Materials Science, Siberian Branch of Russian Academy of Science, Akademichesky ave., 2/4, 634021 Tomsk, Russia.
E-mail address: astafe@ispms.tsc.ru (E.G. Astafurova).

Hadfield steel (Fe-13.7Mn-1.3C wt%) single crystals were grown by the Bridgman technique in an inert gas atmosphere. All crystals were then homogenized in an argon atmosphere at 1373 K for 24 h, solution-treated and water-quenched from 1373 K after 1 h. Following the heat treatment an 0.5 cm thick layer was removed from the crystal to get rid of decarburization and Mn-depletion effects. Next, electro-discharge machining was utilized to cut regular dog-bone shaped flat tensile specimens with nominal dimensions of 15 mm × 2.8 mm × 0.5 mm in the gauge section. The deviation of the specimen tensile axis from the ⟨001⟩ and ⟨111⟩ orientations did not exceed 5°. Mechanical grinding and a final electrochemical polish (50 g CrO_3 in 200 g H_3PO_4) were employed to remove the entire processing-affected surface layer.

The single crystals were electrochemically charged at a current density of 10 mA/cm² for 1 and 5 h at room temperature in 3% NaCl water solution containing 3 g l^{-1} of NH_4SCN as a recombination poison. An austenitic stainless steel was used as counter electrode. Prior to testing, the hydrogenated specimens were stored in liquid nitrogen. Hydrogen content was measured by inert gas fusion thermal conductivity detection (LECO RHEN 602 analyzer). The hydrogen content was measured to be 2.8 wt. ppm for hydrogen-free, 8.4 wt. ppm for 1 h-charged and 13.7 wt. ppm for the 5 h-charged specimens. The tensile tests were conducted at room temperature at an initial strain rate of 5.6×10^{-4} s^{-1} using an electromechanical machine (LFM-125 from Walter + Bai AG). The true strain was calculated based on the data obtained from a video-extensometer. True stress was calculated considering the variation in cross-section area based on the assumption of a constant volume of the specimen. For microstructural analysis, a JEM2100 transmission electron microscope (TEM) operated at an accelerating voltage of 200 kV was employed. Dislocation density in the deformed specimens was calculated using TEM images obtained under different diffraction conditions. For each zone axis, the measured dislocation density was then corrected for the known fraction of invisible dislocation as described in [17].

Fig. 1 shows the true stress – true strain curves and microstructures at 10% strain for ⟨001⟩ and ⟨111⟩ -oriented single crystals of Hadfield steel in the hydrogen-free condition. Hydrogen charging up to 5 h did not substantially change the macroscopic plastic flow behavior and deformation mechanisms of the single crystals nor did it promote any phase transformations in the Hadfield steel. Deformation of ⟨001⟩ -oriented single crystals both in the
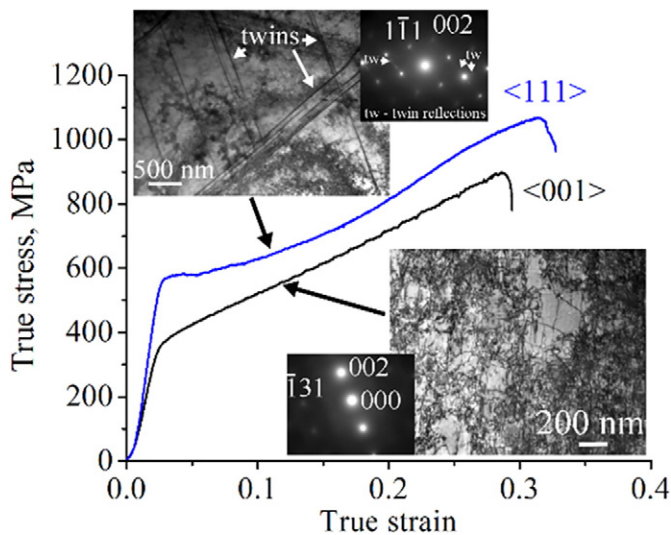
hydrogen-free and hydrogen-charged cases is associated with a/2 ⟨110⟩ {111} dislocation slip and a rather homogeneous distribution of dislocations was observed in the microstructure at 10% strain (Fig. 1). For ⟨111⟩ -oriented single crystals, multiple twinning occurred along with dislocation slip (Fig. 1). At 10% strain, the average dislocation densities for both orientations were similar, i.e. $\rho \approx 4 \times 10^{14}$ m^{-2} (Table 1). Taking into account the $4\sqrt{D_V t}$-criterion and $D_v = 7.37 \times 10^{-16}$ m²/s for austenite at room temperature [18], the depth of the hydrogen-affected zone can be estimated to be about 9 and 15 μm immediately after hydrogen charging for 1 and 5 h, respectively. Clearly this is <10% of the specimen thickness, and a inhomogenous hydrogen distribution might be expected. However, the actual relaxation and aging experiments were performed after 10% straining of the crystals, and the moving dislocations contribute substantially to hydrogen transport. In fact in TEM, there was no visible difference in dislocation arrangement between the surface layer (down to about 20 μm from the surface) and the central part of 10% strained hydrogen-charged specimens. Moreover, the fractographic appearance was similar throughout the specimen thickness. Therefore, it is justified to assume that the hydrogen distribution is almost homogeneous at 10% strain due to strain-induced and defect-accelerated diffusion.

Fig. 2a and b show the result of stress relaxation and reloading tests in ⟨111⟩ and ⟨001⟩ -oriented single crystals, respectively. The stress relaxation and reloading involved the following steps: The specimens were deformed at the initial strain rate of 5.6×10^{-4} s^{-1}. At ≈10% strain, the deformation was stopped and the stress drop $\Delta\sigma_1$ was recorded. After relaxation for 180 s, the specimens were reloaded with the same strain rate. To describe strain-aging, the yield peak $\Delta\sigma_2$ (stress increment) and the time τ needed for plastic flow behavior to return to the initial monotonic loading response, were recorded. For visualization of the values $\Delta\sigma_1$, $\Delta\sigma_2$ and τ see inset to Fig. 2a.

During the relaxation phase, there is a substantial decrease in stress for both types of crystal orientations (Fig. 2a–b). The stress decreases rapidly from its initial value, σ_R, in the first tens of seconds and then slowly and approaches a steady-state value (Fig. 2 c). After relaxation, the characteristic dislocation arrangement for the ⟨111⟩ -oriented crystals was still similar to the one observed in 10% strained and directly unloaded specimens. However, the dislocation density decreased by a factor of 2 down to $\rho \approx 2 \times 10^{14}$ m^{-2} and dislocation-free cells formed (Fig. 3).

The values of the stress drop $\Delta\sigma_1$ for ⟨111⟩ -oriented crystals are higher than those for the ⟨001⟩ -oriented crystals. This was observed both for the hydrogen-free and the hydrogen-charged conditions (Table 1, Fig. 2c). Moreover, hydrogen charging promotes an increase in $\Delta\sigma_1$-value in the twinning-assisted ⟨111⟩ -oriented crystals, but does not influence it in the ⟨001⟩ -oriented single crystals, cf. Fig. 2c. Following the approach of Abracham and Altstetter [6], the stress relaxation rate has been plotted versus reciprocal time in Fig. 2d. Clearly, hydrogen charging influences the stress relaxation rate of single crystals in different ways, i.e. it increases it for the ⟨001⟩ -oriented crystals and decreases it for the ⟨111⟩ case.

The plastic strain rate $\dot{\varepsilon}$ during relaxation can be calculated from the stress relaxation rate $\dot{\sigma} = d\sigma/dt$ via $\dot{\varepsilon} = -\frac{\dot{\sigma}}{M}$, where M is the effective modulus of the sample-machine system [6,19]. From Fig. 2d, the ratio of the plastic strain rates, $\frac{\dot{\varepsilon}^{<111>}}{\dot{\varepsilon}^{<001>}} = \frac{\dot{\sigma}^{<111>}}{\dot{\sigma}^{<001>}}$, is about 3 for the hydrogen-free crystals during the first 10 s of relaxation. As hydrogen has different effects on strain rate during relaxation for the two crystal orientations, this ratio becomes smaller upon hydrogen charging. Still, the value of $\frac{\dot{\varepsilon}^{<111>}}{\dot{\varepsilon}^{<001>}}$ is in the interval from 3 to 2 for the 5 h charging case.

Stress relaxation is a result of the stress-induced motion of mobile dislocations. Dislocation densities at 10% strain and the corresponding stress level σ_R were similar for both orientations during the relaxation tests (Table 1). Thus, the experimentally observed differences in the

Fig. 1. True stress – true strain curves and TEM microstructures corresponding to 10% strain for ⟨001⟩ - and ⟨111⟩ -oriented Hadfield steel single crystals at room temperature.